REVIEW ARTICLE

Quantitative parametric MRI of articular cartilage: a review of progress and open challenges

[1,2]D A BINKS, PhD, [2]R J HODGSON, PhD, FRCR, [3]M E RIES, PhD, [1,2]R J FOSTER, PhD, [2,4]S W SMYE, PhD, [1,2]D MCGONAGLE, PhD, FRCPI and [1,2]A RADJENOVIC, PhD

[1]Section of Musculoskeletal Disease, Leeds Institute of Molecular Medicine, University of Leeds, Leeds, UK
[2]National Institute for Health Research, Leeds Musculoskeletal Biomedical Research Unit, Chapel Allerton Hospital, University of Leeds, Leeds, UK
[3]Polymer and Complex Fluids Group, School of Physics and Astronomy, University of Leeds, Leeds, UK
[4]Academic Division of Medical Physics, University of Leeds, Leeds, UK

Address correspondence to: Dr Aleksandra Radjenovic
E-mail: a.radjenovic@leeds.ac.uk

ABSTRACT

With increasing life expectancies and the desire to maintain active lifestyles well into old age, the impact of the debilitating disease osteoarthritis (OA) and its burden on healthcare services is mounting. Emerging regenerative therapies could deliver significant advances in the effective treatment of OA but rely upon the ability to identify the initial signs of tissue damage and will also benefit from quantitative assessment of tissue repair *in vivo*. Continued development in the field of quantitative MRI in recent years has seen the emergence of techniques able to probe the earliest biochemical changes linked with the onset of OA. Quantitative MRI measurements including T_1, T_2 and $T_{1\rho}$ relaxometry, diffusion weighted imaging and magnetisation transfer have been studied and linked to the macromolecular structure of cartilage. Delayed gadolinium-enhanced MRI of cartilage, sodium MRI and glycosaminoglycan chemical exchange saturation transfer techniques are sensitive to depletion of cartilage glycosaminoglycans and may allow detection of the earliest stages of OA. We review these current and emerging techniques for the diagnosis of early OA, evaluate the progress that has been made towards their implementation in the clinic and identify future challenges in the field.

The treatment of the degenerative joint disease osteoarthritis (OA) remains problematic. For advanced end-stage "whole organ" disease the only viable treatment option is joint replacement where feasible. For earlier stage OA, disease progression is unpredictable and often slow, which makes it very difficult to evaluate agents that have possible disease-modifying properties. Although the OA disease process may commence within any joint structure including ligaments, bone, meniscus or articular cartilage, the advancement of disease is inevitably associated with progressive cartilage attrition and inexorable functional deterioration. The non-invasive assessment of tissue damage (at a stage in the disease process where tissue damage is potentially reversible) and the ability to monitor its repair during and following treatment is central to the future development of novel therapies aimed at arresting or reversing cartilage destruction.

The purpose of this review is to evaluate current and emerging quantitative MR protocols for assessment of cartilage in order to identify the open challenges that will drive further development in the field. Of specific interest are the methods that can detect the initial stages of cartilage degradation and also those that allow the biomechanical properties of cartilage to be studied. Such techniques might be important aids for early diagnosis of arthritic diseases and also in assessing the

Figure 1. (a) The macromolecular composition of cartilage. The collagen fibril network provides the structural framework for cartilage and confers resistance to shear and tensile forces. Proteoglycans are embedded within the collagen network and consist of a central protein core and covalently attached negatively charged glycosaminoglycan (GAG) side chains. The negatively charged GAGs increase the local concentration of cationic species such as Na^+ and help to maintain fluid within the tissue, bestowing stiffness and resistance to compressive forces. (b) In proteoglycan-depleted cartilage, the loss of negatively charged GAGs and the corresponding reduction in mobile cation concentration diminish the ability of the cartilage macromolecular matrix to constrain fluid, reducing its capacity to withstand compression.

proteoglycan / GAG side-chains
collagen fibril network
water / electrolytic fluid
charge balancing cations

progress of regenerative and reparative therapies for OA *in vivo* [1,2]. An ideal scenario would be the development of high-resolution whole body MRI methods that could provide functional information about the state of cartilage at multiple sites, in a timely and cost-effective fashion, without resort to exogenous contrast agents. This is particularly challenging for the assessment of cartilage because high spatial resolution is required. We will discuss what degree of progress has been made towards that lofty goal where MRI biomarkers could be used to reliably identify and characterise early cartilage damage or sites at risk of cartilage loss.
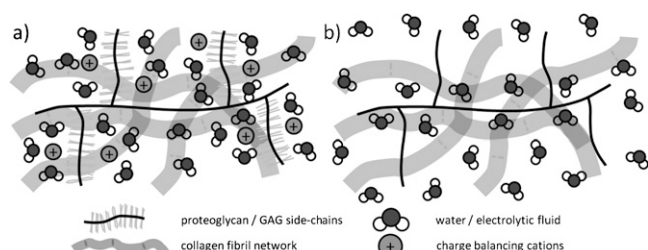
CARTILAGE COMPOSITION

The purpose of articular cartilage is to provide a wear-resistant, low-friction, force-distributing material between the comparatively rigid subchondral bone surfaces in diarthrodial joints. At a macromolecular level cartilage consists of an extracellular matrix (ECM) made up of a network of collagen fibrils and proteoglycan (PG) molecules [3]. PG itself consists of a protein core with covalently attached negatively charged glycosaminoglycans (GAGs). This macromolecular matrix accounts for around 20–30% of the tissue weight. The rest is made up of fluid, containing mobile charge-balancing cationic species [4] (Figure 1a). The mechanisms by which the electrolytic fluid, collagen network and PG molecules interact with each other confer on articular cartilage its biomechanical properties and allow it to withstand and distribute the various forces experienced during joint articulation. Early osteoarthritic changes in articular cartilage occur in the ECM with loss of PG accompanied by heightened water content [5]. The loss of PG and, therefore, negative fixed charge density (FCD) results in increased water mobility in the cartilage matrix and a diminished capacity to cope with mechanical loading (Figure 1b). This in turn exposes the cartilage to further degradation. Thus, there is a great deal of interest and merit in searching for diagnostic techniques that are sensitive to the earliest microscale biochemical changes associated with cartilage degradation and OA [2].

MRI OF CARTILAGE

Since its introduction into clinical practice in the 1980s, MRI has become a powerful and capable diagnostic tool, and excels in its ability to acquire images with a high degree of soft-tissue contrast non-invasively and in three dimensions [6]. Image contrast can be varied through choice of imaging parameters in order to

emphasise different types of tissue. In conventional MRI sequences, contrast is typically afforded by making the signal intensity of each pixel in the image partially dependent upon—or "weighted" by—either the T_1 or the T_2 relaxation time of the hydrogen nuclei contained within that pixel. The T_1 and T_2 relaxation times of nuclei are determined by their physiochemical environment and can thus vary between different tissue types. MR sequences in which both T_1 and T_2 weighting are minimised are said to be proton density weighted, meaning that the signal is determined almost solely by the local concentration of hydrogen nuclei.

MRI is already widely used in the clinic for assessment of articular cartilage and gross joint morphology as well as for the identification of other arthritic features including osteophytes, bone marrow oedema and meniscal and ligament tears [7–10]. The need to differentiate between articular cartilage and a range of surrounding tissue types (bone, muscle, fat, synovial fluid etc.) has meant that a number of MR pulse sequences are used in a typical clinical assessment (Figure 2). The design of the National Institutes of Health Osteoarthritis Initiative knee MRI protocol [7] serves to highlight the variety of sequences implemented; the protocol includes sequences with T_1 weighted, T_2 weighted and intermediate-weighted contrasts using both spin echo and gradient recalled echo methods. Imaging planes are prescribed in sagittal and coronal directions and two-dimensional and three-dimensional (3D) images are acquired, with the latter allowing for images to be reconstructed in multiple planes. The entire protocol is designed to be performed in a relatively short timeframe with respect to patient comfort and allows quantitative and semi-quantitative assessments of a multitude of structural features and pathologies within the knee joint.

Advances in the design of superconducting magnets have facilitated scanners and spectrometers with stronger static magnetic (B_0) fields, allowing for imaging with a combination of increased signal-to-noise ratio (SNR), higher spatial resolution and accelerated acquisition time. Experimental narrow-bore magnets with field strengths of 9.4 and 11.7T are common, while whole body scanners with 3.0-T fields are becoming more prevalent in clinical settings [11]. Similarly, progress in imaging pulse sequence design and development of more sensitive and sophisticated radiofrequency (RF) coils has led to MRI techniques that are able to directly assess the microscopic structure and biochemical composition of musculoskeletal tissues in addition to imaging macroscopic structural and anatomical detail. The capacity to determine microscopic structure and composition is a key factor for the diagnosis of OA because macroscopic degenerative changes (e.g. cartilage defects or joint space narrowing) are usually absent in the early stages of the disease [12]. Moreover, gross structural changes with joint malalignment may not be amenable to putative therapies [13]. The remainder of this review will focus on emergent quantitative MRI techniques that allow this microscopic assessment of articular cartilage.

Figure 2. Conventional parameter-weighted MR images of a cadaveric knee joint. (a) Two-dimensional coronal intermediate-weighted spin echo image used to assess gross joint alignment, collateral ligaments and medial and lateral menisci, as well as cartilage morphology and the presence or absence of subchondral cysts. (b) Three-dimensional (3D) T_2* weighted gradient echo image with selective water excitation; a 3D acquisition which allows the cartilage thickness and volume to be measured as well as providing information about bone attrition and osteophyte formation.


(a)   (b)
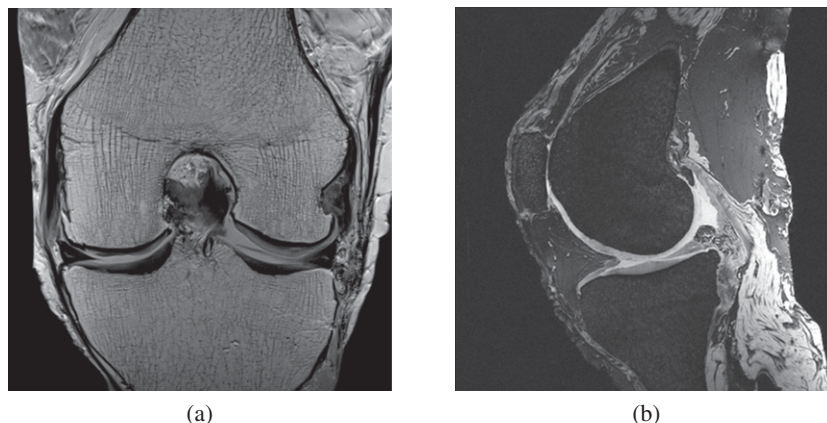
T_1 RELAXATION

Whereas signal intensity in the weighted imaging sequences briefly introduced above is a function of the concentration (spin density) and one or more intrinsic properties (*e.g.* T_1, T_2) of the imaged nuclei, the aim with quantitative MRI techniques is to survey or "map" the absolute value of these intrinsic properties on a pixel-by-pixel basis (Figure 3).

The spin lattice or T_1 relaxation time governs the rate at which nuclei return energy to their surroundings (the "lattice") following excitation [14]. The factors affecting native T_1 relaxation times in articular cartilage are not well understood, although it has been reported that native T_1 values are sensitive to the macromolecular structure of the cartilage matrix [15]. The exact nature of this relationship is unclear, but is believed to relate more to the PG content of the tissue than the collagen architecture [16]. A systematic survey of native T_1 in different cartilage compartments of healthy human volunteers was undertaken by Wiener et al [17]. In this study, T_1 values were shown to decrease from the superficial cartilage layers to the deep layer, consistent with the dependence of native T_1 values upon the macromolecular construction of cartilage.

Figure 3. Quantitative MR parameter mapping. A pixel-by-pixel map of a single MR property is displayed on top of an anatomical image, showing the variation of that particular parameter in a region of interest. This particular image shows the variation in T_2 relaxation time in the femoral articular cartilage and patellar cartilage of the knee joint.
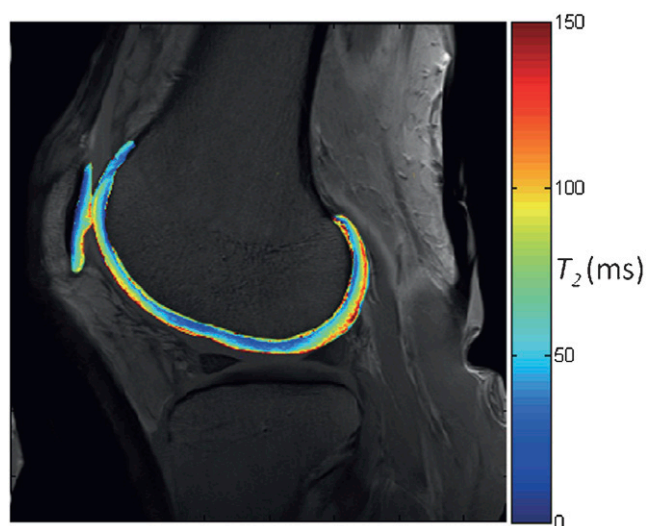

CONTRAST ENHANCED T_1–DELAYED GADOLINIUM-ENHANCED MRI OF CARTILAGE

The studies described in the previous section are concerned primarily with the native T_1 relaxation time of cartilage. An area which has received considerably more attention is the mapping of the T_1 relaxation time of cartilage in the presence of the gadolinium contrast agent gadolinium diethylenetriamine penta-acetic acid [Gd(DTPA)$^{2-}$)]. This forms the basis of the delayed gadolinium-enhanced MRI of cartilage (dGEMRIC) technique [18]. The distribution of the negatively charged contrast agent is inversely proportional to the cartilage FCD owing to the presence of negatively charged GAG side chains on PG (Figure 4). Areas of cartilage with depleted GAG concentration therefore accumulate more contrast agent. The highly paramagnetic gadolinium ions promote relaxation processes, leading to a localised reduction in the T_1 relaxation time. dGEMRIC can, therefore, be used to determine the spatial variation of tissue GAG concentration and is a technique that shows promise as a specific measure of early degradation in the cartilage ECM associated with OA [19]. In a clinical setting, there is support for the efficacy of the technique for detecting pre-radiographic signs of OA in the knee [20] and hip [21] joints.

A number of practical considerations relating to the *in vivo* implementation of the dGEMRIC technique have been investigated and addressed by Burstein et al [22]. The relationship between the contrast-enhanced T_1 and GAG concentration is subject to effective penetration of the contrast agent into the cartilage, which may be affected by a patient's body mass index (BMI) and/or ratio of fat to lean tissue. They recommend intravenous injection of a double dose ($0.2 \, \text{mmol} \, \text{kg}^{-1}$) of Gd (DTPA)$^{2-}$, followed by a 10-min period of exercising the joint to aid penetration of the contrast agent into the cartilage. Maximum contrast is achieved 2h post injection for the knee joint. A separate study reports that complete equilibration of Gd(DTPA)$^{2-}$ throughout the entire thickness of the cartilage may take as long as 12h [23]. Additionally, the direction and type of loading experienced by the joint during the exercise period may affect the distribution of the contrast agent [24].

A further consideration for dGEMRIC is whether both pre- and post-contrast T_1 values are required to

Figure 4. Distribution of gadolinium diethylenetriamine penta-acetic acid $[Gd(DTPA)^{2-}]$ in (a) healthy and (b) glycosaminoglycan (GAG)-depleted cartilage extracellular matrices. The local concentration of the administered gadolinium contrast agent is inversely proportional to cartilage GAG content owing to the electrostatic repulsion between negatively charged GAGs and the negatively charged contrast agent. Water proton T_1 relaxation times are reduced in the vicinity of the paramagnetic contrast agent and can therefore be used to measure GAG concentration.
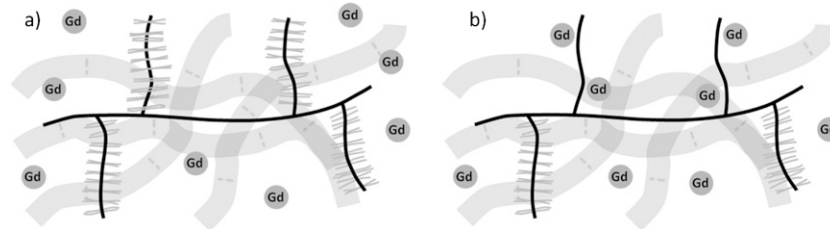
accurately evaluate variations in cartilage GAG content [1,25–27]. Where only the post-contrast T_1 is used to report the so-called dGEMRIC index, the assumption has been made that the pre-contrast value of T_1 (T_{10}) is relatively constant and that the post-contrast value of T_1 is sufficiently small compared with T_{10}. The current consensus is that the post-contrast T_1 gives a sufficiently accurate measure of GAG concentration and the time-consuming measurement of pre-contrast T_1 is not necessary [28].

Apart from these concerns, there is a desire to implement faster T_1 mapping protocols with higher resolution and 3D joint coverage. This would be beneficial for *in vitro* and *in vivo* studies alike because quantitative T_1 mapping techniques are typically time consuming. This is increasingly relevant at higher field strengths where T_1 relaxation times increase, resulting in even longer scan times [29]. Accurate 3D T_1 mapping protocols have been implemented on 1.5- and 3.0-T platforms using 3D inversion–recovery spoiled gradient echo [29], 3D Look–Locker [30] and 3D fast two-angle T_1 mapping [31] methods.

T_2 RELAXATION

T_2 relaxation concerns the loss of phase coherence between nuclei following excitation by an RF pulse. Immediately after the excitation, nuclei have phase coherence resulting in a detectable net magnetisation vector [14]. As T_2 relaxation occurs, this phase coherence is lost and the observable nuclear magnetic resonance (NMR) signal decays exponentially with time. In cartilage, the restricted motion of water molecules imposed by the macromolecular structure of the ECM promotes relaxation, resulting in shorter T_2 relaxation times [1]. T_2 relaxation times are therefore dependent

on both the water content and the condition of the surrounding macromolecular structure [32]. Increased hydration of cartilage and breakdown of cartilage collagen are both early indicators of osteoarthritic disease [5]; therefore, there is considerable interest in the potential for T_2 as a predictor of early OA [33]. Early work in this area was conducted by Dardzinski et al [34] in a study of seven asymptomatic adults. Cartilage T_2 relaxation times were shown to vary across the thickness of the cartilage in a manner consistent with the known spatial distribution of cartilage water and PG content. The erosion of the cartilage ECM and increased tissue water content associated with degraded tissue is generally linked to higher T_2 values. Dunn et al [35] reported on the correlation between increased T_2 values and severity of OA in a study of 55 patients. Subjects with mild and severe OA had significantly higher cartilage T_2 values than those who were healthy. A study of the Osteoarthritis Initiative patient cohort [36] showed a link between heightened T_2 values of patellar cartilage and knee abnormalities. It has, however, been suggested that explicit interpretation of changes in T_2 should be made with care, owing to the number of competing biological and mechanical effects that influence T_2 [1].

The effect of collagenous architecture on T_2 relaxation times is evident in the zonal variation of T_2 values in the deepest cartilage layers adjacent to the bone and in the tangential zone cartilage at the articular surface. In the deep and tangential layers of articular cartilage where the orientation of collagen fibrils is anisotropic, T_2 values show a dependence on the alignment of the cartilage with the B_0 field [37,38]. This dependence is not observed in the intermediate cartilage layer where there is a random distribution of collagen fibril orientations. The effect on T_2 values arises because of the

so-called magic angle effect [14], whereby the dipole–dipole interactions between nuclei that promote relaxation are minimised when the angle between the internuclear vector and the B_0 field is 54.7°. While it is apparent that T_2 values in cartilage are strongly influenced by collagen architecture, with a study by Nissi et al [39] suggesting that 60% of the variation in T_2 values can be rationalised by changes in the collagen fibril orientation, the remaining 40% is then determined by other factors including water content [40] and concentration of other macromolecules [41]. This reiterates the need for care in interpreting variations in T_2 relaxation times.

A further consideration for evaluation of cartilage T_2 relaxation times is the need for MR pulse sequences that are able to probe tissues with short (<10ms) T_2 values, including calcified cartilage and fibrocartilage [42]. Ultrashort echo time (UTE) MRI sequences are sensitive to these very short relaxation times and allow for quantitative assessment of the highly organised collagen network, particularly in the deep and calcified cartilage zones [43].

$T_{1\rho}$ RELAXATION

The spin lattice relaxation time in the rotating frame ($T_{1\rho}$) is sensitive to low-frequency exchange interactions between water molecules and the large, slow tumbling macromolecules that constitute the cartilage ECM [33]. $T_{1\rho}$ measurements are performed using a preparatory spin locking pulse that attenuates T_2 relaxation and causes the magnetisation to evolve according to the $T_{1\rho}$ relaxation time of the nuclei [44]. Following the spin-locked preparation of the magnetisation, spatial encoding of the NMR signal can be achieved using standard sequences, including spin echo [45] and gradient echo [46,47]. Variation of the pulse duration allows points on the $T_{1\rho}$ decay curve to be sampled and the $T_{1\rho}$ relaxation time to be determined.

$T_{1\rho}$ measurements have been shown to be sensitive to changes in PG content in enzymatically degraded bovine cartilage [45,48], indicating the potential for $T_{1\rho}$ to be used as a biomarker for the early stages of OA. A more recent study examined the ability of quantitative $T_{1\rho}$ measurements to identify cartilage degeneration as validated by arthroscopic investigation, with $T_{1\rho}$ showing the potential to identify cartilage with softening and swelling corresponding to a Grade I

classification on the Outerbridge scale used for visual assessment of chondral lesions [49]. Evaluation of cartilage repair in patients undergoing microfracture and mosaicplasty surgical procedures was also performed [50] using $T_{1\rho}$.

Several studies compared the relative sensitivities of quantitative $T_{1\rho}$ and T_2 measurements to the earliest degenerative changes in the cartilage ECM [51,52]. The consensus was that $T_{1\rho}$ may be more sensitive to the initial changes in the cartilage ECM associated with PG depletion, whereas T_2 is sensitive only to later changes in the collagen network. Furthermore, the relative change in $T_{1\rho}$ values in healthy *vs* degenerative tissue is larger than for T_2, offering an improvement in dynamic range for detecting early OA pathology [53]. It has also been shown that $T_{1\rho}$ values appear to be unaffected by the laminar structure of cartilage [54].

There are still conflicting opinions on the specificity of $T_{1\rho}$ measurements for measuring PG content [1,44,55] because $T_{1\rho}$ may be at least partially susceptible to the same competing factors that limit the specificity of T_2 measurements, such as tissue collagen content and hydration. The availability of standard clinical $T_{1\rho}$ pulse sequences can also be problematic [1]. Additionally, the long duration of the spin locking pulse means that large amounts of RF energy are transmitted to the subject during the pulse sequence, and this must be controlled within prescribed limits for safe use on patients [44]. This is particularly pertinent at higher field strengths because the RF energy transmitted for any discrete excitation increases with the square of the field strength [56].

RELATIONSHIP BETWEEN MECHANICAL PROPERTIES OF CARTILAGE AND QUANTITATIVE MRI

Owing to the sensitivity of certain MR techniques to the macromolecular structure and content of articular cartilage, there is a related interest in the prediction of the mechanical properties of cartilage using these non-invasive MRI methods. Continued development of such methods could have a significant impact on the ability to inform biotribological studies of articular cartilage wear and degeneration [57,58].

Nissi et al [15] attempted to determine the relationship between the mechanical properties of human, bovine and porcine patellar cartilage and MR parameters of the

tissue. Native T_1 and T_2 values and dGEMRIC were measured along with Young's modulus and the dynamic modulus of the samples. Lower native T_1 relaxation times were found in tissue with high stiffness, possibly reflecting the reduced water content and high concentration of collagen and PG in such areas. The relationship between stiffness and T_2 values was less clear. Differences in the laminar structure of the cartilage samples relating to the varying stages of maturity presented a complex relationship between stiffness and bulk T_2 values. However, a significant correlation was observed when data for human, bovine and porcine cartilage were pooled together. Somewhat surprisingly, given the relationship between dGEMRIC and PG content, the study did not find any significant correlation between the measured mechanical properties and contrast-enhanced T_1 values. This was attributed to the dominating effect of the collagen architecture to which dGEMRIC is insensitive. Juras et al [59] later reported a high correlation between contrast-enhanced T_1 values and the instantaneous and equilibrium modulus values of human cartilage explants. This study also reiterated the difficulty in correlating T_2 with stiffness values.

The sensitivity of $T_{1\rho}$ measurements to PG content was exploited by Wheaton et al [60] in an attempt to measure the mechanical properties of cartilage using MRI. In this work, changes in the $T_{1\rho}$ relaxation time were shown to correlate with both the PG content, as determined by spectrophotometric assay, and the compressive modulus and hydraulic permeability of bovine cartilage samples.

More recent work by the group from the University of Kuopio [16,61] involved the development of a finite element model (FEM) from which the mechanical properties of cartilage can be inferred from MR parameters and other complementary methods, e.g. infrared imaging and polarised light microscopy. This work concludes that an FEM can enable the mechanical properties of cartilage to be inferred, given the depth-dependent collagen content, the PG and water content and the collagen architecture. MR techniques can determine water and PG content and collagen architecture, but not the collagen content.

SODIUM MRI

Sodium MRI offers an alternative method to dGEMRIC for the measurement of cartilage FCD. Negative FCD in the cartilage ECM is charge balanced by the presence of positively charged sodium ions (Figure 5). Thus, determination of the concentration of sodium within the tissue allows the negative FCD, and hence GAG concentration, to be quantified [44]. The first evidence of the suitability of sodium MRI for this type of measurement was presented as far back as 1988 [62]. Gradient echo MR images of various tissues, including cartilage, were obtained at 1.9T with moderate acquisition times (2–30min). As with the dGEMRIC method, measurement of FCD using sodium MRI is highly specific to the GAG concentration but, importantly, does not require the use of a contrast agent; intravenous administration of contrast agent is invasive and potentially uncomfortable for the patient, prolongs the examination time and has been associated with increased risk of nephrogenic fibrosing dermopathy [63]. Several reports [64–66] later demonstrated the specificity of the technique for detecting cartilage degradation through small changes in the FCD, along with improvements in image quality and speed of image acquisition. Clinical studies of cartilage using sodium MRI remain comparatively rare, hampered by the technical difficulties of obtaining sufficient signal to noise in a clinically relevant timeframe.

Figure 5. Distribution of sodium (Na^+) ions in (a) healthy and (b) glycosaminoglycan (GAG)-depleted cartilage extracellular matrices. The negative fixed charge density of GAG is balanced by cationic Na^+ ions. GAG-depleted regions have lower negative fixed charge densities and therefore fewer Na^+ ions. MRI techniques can measure the Na^+ concentration, allowing the fixed charge density and GAG concentration to be calculated.
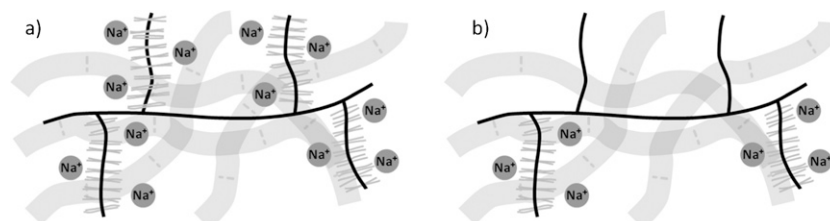
The major challenges involved in sodium MRI arise as a result of the inherently lower concentration of ^{23}Na nuclei in the cartilage ECM and a smaller gyromagnetic ratio than the ^{1}H nucleus. The T_1 and T_2 relaxation times of sodium are also comparably short. Combined, these factors have an impact on the achievable SNR and image resolution using the technique [44]. Signal loss due to rapid T_2 relaxation can be offset by the use of UTE sequences [67]. Indeed, a precise measurement of sodium concentration using sodium MRI necessitates the use of UTE or similar sequences owing to the rapid T_2 relaxation rate of the sodium nucleus [44]. SNR enhancement is also facilitated through the use of radial k-space acquisition trajectories [68,69], where the NMR signal is acquired immediately after excitation from the centre of the k-space and therefore does not undergo decay during the phase-encoding steps required in a conventional Cartesian k-space trajectory.

MAGNETISATION TRANSFER

In a conventional MRI sequence, it is the hydrogen nuclei of unbound bulk water molecules that contribute to the observed signal. In a magnetisation transfer sequence, a preparatory saturation pulse is applied prior to the main MR sequence which excites the broad signal of less mobile macromolecule-bound water molecules (Figure 6a). Exchange between the two water pools results in an attenuation of the bulk water signal, the extent of which depends on the kinetics of the exchange process and the volume of the bound water pool [70]. Magnetisation transfer contrast is therefore used to

highlight interactions between the bulk water and macromolecules (bound water). The extent of magnetisation transfer is often expressed as the magnetisation transfer ratio (MTR), which is simply the ratio of signal intensities observed with and without the application of the preparatory saturation pulse. An alternative metric is the rate constant for exchange of water between the two pools [71].

For cartilage imaging, the important magnetisation transfer interaction is between bulk water and water bound to the collagen fibres present in the cartilage ECM, although there is also a contribution from PG [72–75]. Regatte et al [72] investigated the depth dependence of MTR values in bovine cartilage samples and observed higher MTRs in the deep cartilage zone. This was attributed to the depth-wise variation in cartilage collagen content as well as variations in the radial orientation of collagen fibrils and variations in the bound water fraction throughout the thickness of the cartilage. Yao et al [76] reported on the insensitivity of MTR measurements to early degenerative changes in cartilage, also suggesting that the dependence of the MTR on multiple factors makes variation in MTRs difficult to interpret.

A recent development of the magnetisation transfer principle is the chemical exchange-dependent saturation transfer (CEST) technique [77]. Exchangeable protons of a solute are selectively excited and chemical exchange of these protons with water protons results in a detectable decrease in the magnetisation of the bulk water pool [78] (Figure 6c). By saturating hydroxyl

Figure 6. Saturation transfer effects between protons in the free and bound water pools and exchangeable protons of solute molecules. (a) In magnetisation transfer (MT), an off-resonance radiofrequency (RF) pulse saturates the broad proton resonance of low-mobility bound water molecules. Proton exchange between bound water molecules and the free water pool results in saturation transfer to the free water pool and a detectable reduction in the signal intensity of the free water resonance. (b) The magnetisation transfer ratio (MTR) is defined as MTR$=1-S_{MT}/S_O$, where S_O is the signal intensity recorded without a preparatory saturation pulse and S_{MT} is the signal intensity observed with the inclusion of a preparatory saturation pulse. (c) In the chemical exchange-dependent saturation transfer (CEST) technique, solute protons are selectively saturated by using an RF pulse. Chemical exchange of the solute protons with water protons again results in saturation transfer to the free water pool and a measurable reduction in water proton signal intensity.
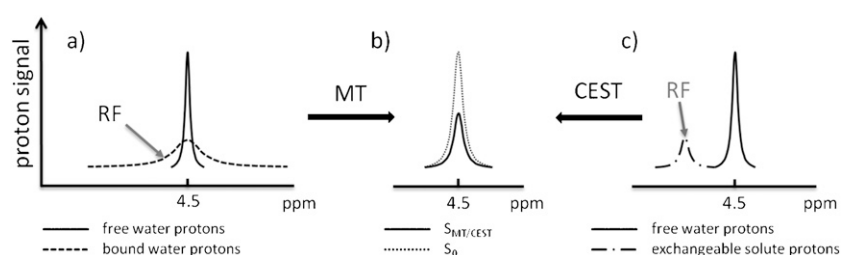
residues of GAG (Figure 7), the CEST effect can be exploited to directly measure GAG content *in vivo* [79]. In this study by Ling et al [79], the GAG-CEST technique was implemented *in vivo* on a 3-T clinical scanner and was able to show the demarcation of a cartilage lesion in a human knee joint. Schmitt et al [80] compared the GAG-CEST technique with sodium MRI in a study performed at 7 T on patients who had undergone cartilage repair surgery, with a high correlation observed between the two techniques.

DIFFUSION MRI

Diffusion MRI techniques are sensitive to the restriction of motion of water molecules bound within a macromolecular environment. Diffusion-sensitive MRI methods use paired magnetic field gradient pulses to probe the motion of nuclei in the direction of the applied magnetic field gradient [81]. The two pulses are of equal duration and amplitude and are separated by a time delay (Δ). The net effect of the paired gradient pulses is to dephase magnetisation from nuclei which have undergone diffusion during the time delay, resulting in a measurable signal attenuation. The measured signal (S) is related to the diffusion coefficient (D) of the nuclei by the Stejskal–Tanner equation (Equation 1) [82]:

$$\frac{s}{s_0} = \exp\left[-\gamma^2 G^2 \delta^2 \left(1\Delta - \frac{\delta}{3}\right)D\right] \tag{1}$$

where γ is the gyromagnetic ratio of the diffusing nuclei, G and δ are the amplitude and duration, respectively, of

Figure 7. Molecular structure of one disaccharide unit of chondroitin-4-sulphate, one of the constituent glycosaminoglycans (GAGs) of proteoglycan. Exchangeable protons that contribute to the chemical exchange-dependent saturation transfer (CEST) effects seen using the GAG-CEST technique are highlighted. H, hydrogen; N, nitrogen; O, oxygen; S, sulphur.

the applied gradient pulses and S_0 is the measured signal intensity when $G=0$. Typically, a diffusion-sensitive MRI sequence consists of a number of diffusion gradient pulses applied along multiple axes as well as imaging gradients for spatial localisation of the signal. It then becomes convenient to summarise the combined influence of the gradients through calculation of the b-factor [83]. The b-factor determines the overall diffusion weighting of a sequence in the same way that the echo time characterises the degree of T_2 weighting. Acquisition of images with multiple b-factors thus allows the diffusion coefficient to be mapped on a pixel-by-pixel basis.

When measuring the diffusion coefficient of water molecules in physiological systems, there is significant interaction between the water molecules and their surrounding environment during the timescale of the experiment, and the parameter measured is the apparent diffusion coefficient (ADC). Consequently, measuring the ADC of water molecules within the cartilage ECM can be used to infer cartilage tissue structure and architecture [84,85], with increased diffusivity linked to structural degradation of the ECM. Diffusion-weighted imaging (DWI) has been demonstrated as a potential method for assessing cartilage degeneration *in vivo* [86] and monitoring its repair following surgery [8,87]. A longitudinal study by Friedrich et al [88] highlighted the ability of DWI to differentiate between healthy and repaired cartilage at different time points after surgery of patients who underwent matrix-assisted autologous chondrocyte transplantation. The authors highlighted the difficulty in obtaining precise measures of the diffusion values, and compared only the relative changes in diffusivity in this study.

Whereas DWI can report the localised average diffusivity, diffusion tensor imaging (DTI) can be used to obtain the directionality of localised diffusion, revealing the orientation of collagen fibrils in the cartilage ECM [89]. DTI has been used to study the effects of compression on the cartilage collagen network [90], and another study reported on the use of ultrahigh field (17.6 T) DTI to inform a finite element simulation of cartilage deformation [91]. At present, though, DTI is unlikely to be applicable for *in vivo* assessment of cartilage, owing to the intensive data analysis required as well as lengthy acquisition times even at high field strengths.
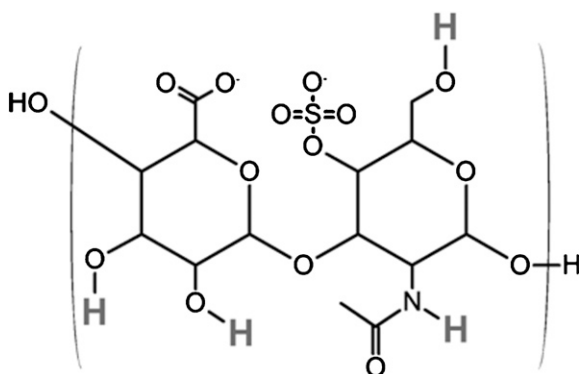
IMAGING OF RELATED MUSCULOSKELETAL TISSUES

The focus so far has been on imaging methods for the assessment of articular cartilage. However, MRI has also been able to show the involvement of related joint structures in the early expression of OA [92,93]. In this study, high-resolution MRI of the hand was carried out using standard clinical protocols on a 1.5-T scanner and compared with histological sections of cadaveric joints. Abnormalities in the collateral ligaments of the distal interphalangeal joint were observed adjacent to sites of bone oedema, bone erosion and new bone formation. In some cases, ligament abnormalities were seen in joints without large-scale loss of cartilage, showing that ligament abnormalities may precede degenerative changes in cartilage in some cases of OA.

The structure of the enthesis organ (the complex arrangement of ligaments and tendons and their interfaces with bone) and its involvement in both inflammatory and degenerative arthritides is also of interest [94,95]. The use of both conventional MR sequences and UTE sequences for visualisation of the enthesis has been studied [42,96], allowing the presence of fibrocartilage to be shown in the enthesis. Previously, histological sectioning has been required to determine the presence of fibrocartilage. UTE sequences are a relatively recent innovation in MRI [97]. Employing imaging sequences with echo times as short as 50 μs allows the signal components with very short T_2 relaxation times to be observed [98], which otherwise decay too rapidly to be observed with standard echo times ($>$5ms). UTE sequences have also enabled magnetisation transfer contrast imaging of tissues with rapid signal decay; Springer et al [99] measured MTRs *in vitro* in bovine cortical bone and *in vivo* in healthy human volunteers, demonstrating the feasibility of the technique for clinical applications.

KEY OPEN QUESTIONS

There is currently significant interest in the identification of biomarkers that would allow for the early detection of OA [2]. There are a number of MR-measurable parameters that have been shown to be sensitive to early biochemical changes, including depletion of GAG and collagen fibre breakdown. The question remains as to which of these parameters are best suited to fulfil the needs of clinicians in making an early diagnosis. For

routine use in a clinical setting, potential imaging techniques should be reliably performed in a relatively short time. Long scanning sessions are uncomfortable for patients and may result in poor quality images owing to patient motion. If the ultimate goal of routine screening of patient groups at risk of developing OA is to be achieved, then completely non-invasive MR methods would be preferable; methods requiring intravenous administration of contrast agents are not only invasive and associated with increased incidence of nephrogenic fibrosing dermopathy but also prolong the examination period, reducing their practicality.

At present, MRI measures of cartilage composition in OA are used predominantly in a research setting to assess potential treatment strategies and to better understand the disease process. Ultimately, the wider clinical applicability of these techniques will depend on the development of new OA treatments, *e.g.* drugs, physiotherapy regimes or minimally invasive surgical procedures. In this context, the ability to detect early cartilage changes (before the development of potentially irreversible structural abnormalities) and assess disease progression and response to treatment would be of potential clinical value. Another key issue for detecting early cartilage changes using MRI would be the targeting of appropriate patient groups at risk of developing OA. Such screening may be based on a variety of predisposing factors, including those associated with certain high-risk occupations and sporting activities as well as previous injury.

MRI methods that are sensitive to the GAG content of cartilage currently represent the most promising opportunities for early non-invasive assessment of cartilage degeneration. Both sodium imaging and dGEMRIC offer a highly specific method of GAG quantification through measurement of tissue FCD. However, the dGEMRIC method requires the use of exogenous contrast agent, making it subject to the disadvantages cited above. Sodium MRI is completely non-invasive but the method is technically demanding, requiring specialist RF coils, pulse sequences and high field strength magnets to obtain useful results. Development of the technique may be stimulated by the increasing presence of clinical 3-T scanners but it may be that even higher field strengths are required.

The specificity and non-invasiveness of the GAG-CEST technique would appear to make it a highly favourable

technique with which to assess GAG content *in vivo*. The feasibility of the technique for *in vivo* studies has been demonstrated [79,80] and the major challenge will be to develop robust CEST pulse sequences suitable for use in a clinical setting.

The potential for $T_{1\rho}$ to provide a completely non-invasive, specific measure of cartilage PG content in a clinically feasible time remains. Further studies on the specificity and sensitivity of the technique are required as well the development and implementation of standardised pulse sequences. These challenges appear to be surmountable in the short-to-medium term and, encouragingly, should be achievable at current clinically available magnet field strengths.

With recent opinion suggesting that OA may initiate in the synovium, ligaments, tendons, menisci and other interrelated joint structures [100,101], the search for imaging biomarkers in these areas may represent an alternative approach to the diagnosis of early OA. Through this approach it may also be possible to obtain important information about the phenotypic expression of OA in general. The study by Tan et al [92] showed that the early involvement of the collateral ligaments in hand OA can be observed using well-developed MRI protocols and currently available equipment. The opportunity exists to translate this approach to other diarthrodial joints including the knee, although full joint coverage at sufficiently high resolution will be more challenging for larger joints. UTE sequences may also be beneficial for the purpose of delineating structures with very short T_2 relaxation times.

Closely related to the search for biomarkers of OA is the desire to infer the mechanical properties of cartilage using quantitative MRI. This would be of benefit to biotribological studies of articulating joints, allowing the effects of mechanical loading to be studied during *in vitro* wear simulations using dynamic MR sequences. The Finnish group at Kuopio/Oulu [16,61] contributed the majority of the research in this area and developed a finite element model of cartilage based on its microscopic composition. Such models will benefit from input of the whole range of quantitative MR parameters discussed here. Much of the microscopic structure and composition of cartilage can be elucidated using MRI: collagen fibril orientation, PG and fluid content; however, the depth-wise variation in collagen content is not yet quantifiable using MRI, and must be obtained using polarised light microscopy or similar techniques.

CONCLUSIONS

Functional assessment of cartilage and other musculoskeletal tissues is possible through the application of a number of quantitative MRI techniques. MRI techniques exist that are sensitive to different aspects of the microanatomical structure of cartilage, including tissue hydration, GAG content and the architecture of the cartilage collagen network.

Quantitative assessment of cartilage GAG content represents perhaps the best opportunity to identify cartilage degradation at its earliest point and there are several MRI techniques that are suitable for this purpose. $T_{1\rho}$ measurement may prove to be the most clinically feasible if the sensitivity and specificity of the parameter for cartilage GAG content can be established. Both dGEMRIC and sodium MRI offer highly specific measurement of GAG content through quantification of FCD, but their clinical implementation may be limited because of the invasiveness of the technique in the case of dGEMRIC and hardware dependency in the case of sodium MRI. Further development of emerging CEST MR methods may allow for direct GAG quantification using the GAG-CEST technique.

Quantitative relaxometry of cartilage offers a less specific assessment of cartilage with native T_1 and T_2 values as well as magnetisation transfer interactions dependent upon a variety of factors not limited to water content and mobility, GAG content and collagen fibril orientation. Further understanding of the macromolecular processes and interactions that determine tissue relaxation times may allow for these phenomenological parameters to be incorporated into computational models able to predict the biomechanical properties of cartilage. Translating MRI parameters into specific mechanical properties of musculoskeletal tissues represents a significant challenge, but the potential benefits to areas of regenerative medicine and biomedical engineering of a means of non-invasive, quantitative assessment are clear.

REFERENCES

1. Burstein D, Gray ML. Is MRI fulfilling its promise for molecular imaging of cartilage in arthritis? Osteoarthritis Cartilage 2006;14: 1087–90.

2. Williams F, Spector T. Biomarkers in osteoarthritis. Arthritis Res Ther 2008;10:101.

3. Buckwalter JA, Mankin HJ. Articular cartilage: tissue design and chondrocyte-matrix interactions. Instr Course Lect 1998;47: 477–86.

4. Mow VC, Holmes MH, Lai WM. Fluid transport and mechanical properties of articular cartilage: a review. J Biomech 1984;17: 377–94.

5. Buckwalter JA, Mankin HJ. Articular cartilage: degeneration and osteoarthritis, repair, regeneration, and transplantation. Instr Course Lect 1998;47:487–504.

6. Gold GE, Chen CA, Koo S, Hargreaves BA, Bangerter NK. Recent advances in MRI of articular cartilage. AJR Am J Roentgenol 2009;193:628–38.

7. Peterfy CG, Schneider E, Nevitt M. The osteoarthritis initiative: report on the design rationale for the magnetic resonance imaging protocol for the knee. Osteoarthritis Cartilage 2008;16:1433–41.

8. Trattnig S, Domayer S, Welsch G, Mosher T, Eckstein F. MR imaging of cartilage and its repair in the knee—a review. Eur Radiol 2009;19:1582–94.

9. Disler DG, Recht MP, McCauley TR. MR imaging of articular cartilage. Skeletal Radiol 2000;29: 367–77.

10. Halstead J, Bergin D, Keenan AM, Madden J, McGonagle D. Ligament and bone pathologic abnormalities more frequent in neuropathic joint disease in comparison with degenerative arthritis of the foot and ankle implications for understanding rapidly progressive joint degeneration. Arthritis Rheum 2010;62:2353–8.

11. Hu X, Norris DG. Advances in high-field magnetic resonance imaging. Annu Rev Biomed Eng 2004;6:157–84.

12. Chan W, Lang P, Stevens M, Sack K, Majumdar S, Stoller D, et al. Osteoarthritis of the knee: comparison of radiography, CT, and MR imaging to assess extent and severity. AJR Am J Roentgenol 1991;157:799–806.

13. Peterfy C, Kothari M. Imaging osteoarthritis: magnetic resonance imaging versus x-ray. Curr Rheumatol Rep 2006;8:16–21.

14. Levitt M. Spin dynamics: basics of nuclear magnetic resonance. New York, NY: Wiley; 2008.

15. Nissi MJ, Rieppo J, Toyras J, Laasanen MS, Kiviranta I, Nieminen MT, et al. Estimation of mechanical properties of articular cartilage with MRI-dGEMRIC, T_2 and T_1 imaging in different species with variable stages of maturation. Osteoarthritis Cartilage 2007;15:1141–8.

16. Julkunen P, Korhonen RK, Nissi MJ, Jurvelin JS. Mechanical characterization of articular cartilage by combining magnetic resonance imaging and finite-element analysis—a potential functional imaging technique. Phys Med Biol 2008;53:2425–38.

17. Wiener E, Pfirrmann CWA, Hodler J. Spatial variation in T_1 of healthy human articular cartilage of the knee joint. Br J Radiol 2010;83:476–85.

18. Bashir A, Gray ML, Burstein D. Gd-DTPA^{2-} as a measure of cartilage degradation. Magn Reson Med 1996;36:665–73.

19. Bashir A, Gray ML, Boutin RD, Burstein D. Glycosaminoglycan in articular cartilage: in vivo assessment with delayed Gd(DTPA)(2-)-enhanced MR imaging. Radiology 1997;205:551–8.

20. Williams A, Sharma L, McKenzie CA, Prasad PV, Burstein D. Delayed gadolinium-enhanced magnetic resonance imaging of cartilage in knee osteoarthritis: findings at different radiographic stages of disease and relationship to malalignment. Arthritis Rheum 2005;52:3528–35.

21. Pollard TCB, McNally EG, Wilson DC, Wilson DR, Madler B, Watson M, et al. Localized cartilage assessment with three-dimensional dGEMRIC in asymptomatic hips with normal morphology and cam deformity. J Bone Joint Surg Am 2010;92: 2557–69.

22. Burstein D, Velyvis J, Scott KT, Stock KW, Kim YJ, Jaramillo D, et al. Protocol issues for delayed Gd(DTPA)(2-)-enhanced MRI: (dGEMRIC) for clinical evaluation of articular cartilage. Magn Reson Med 2001;45:36–41.

23. Silvast TS, Kokkonen HT, Jurvelin JS, Quinn TM, Nieminen MT, Toyras J. Diffusion and near-equilibrium distribution of MRI and CT contrast agents in articular cartilage. Phys Med Biol 2009; 54:6823–36.

24. Mauck RL, Hung CT, Ateshian GA. Modeling of neutral solute transport in a dynamically loaded porous permeable gel: implications for articular cartilage biosynthesis and tissue engineering. J Biomech Eng 2003;125:602–14.

25. Williams A, Mikulis B, Krishnan N, Gray M, McKenzie C, Burstein D. Suitability of T-1Gd as the "dGEMRIC index" at 1.5T and 3.0T. Magn Reson Med 2007;58:830–4.

26. Li W, Du H, Scheidegger R, Wu Y, Prasad PV. Value of precontrast T_1 for dGEMRIC of native articular cartilage. J Magn Reson Imaging 2009;29:494–7.

27. Bittersohl B, Hosalkar HS, Kim YJ, Werlen S, Siebenrock KA, Mamisch TC. Delayed gadolinium-enhanced magnetic resonance imaging (dGEMRIC) of hip joint cartilage in femoroacetabular impingement (FAI): are pre- and postcontrast imaging both necessary? Magn Reson Med 2009;62:1362–7.

28. Trattnig S, Burstein D, Szomolanyi P, Pinker K, Welsch GH, Mamisch TC. T_1 (Gd) gives comparable information as delta T_1 relaxation rate in dGEMRIC evaluation of cartilage repair tissue. Invest Radiol 2009;44:598–602.

29. McKenzie CA, Williams A, Prasad PV, Burstein D. Three-dimensional delayed gadolinium-enhanced MRI of cartilage (dGEMRIC) at 1.5T and 3.0T. J Magn Reson Imaging 2006;24:928–33.

30. Kimelman T, Vu A, Storey P, McKenzie C, Burstein D, Prasad P. Three-dimensional T_1 mapping for dGEMRIC at 3.0 T using the Look Locker method. Invest Radiol 2006;41:198–203.

31. Sur S, Mamisch TC, Hughes T, Kim YJ. High resolution fast T_1 mapping technique for dGEMRIC. J Magn Reson Imaging 2009;30:896–900.

32. David-Vaudey E, Ghosh S, Ries M, Majumdar S. T_2 relaxation time measurements in osteoarthritis. Magn Reson Imaging 2004;22:673–82.

33. Taylor C, Carballido-Gamio J, Majumdar S, Li XJ. Comparison of quantitative imaging of cartilage for osteoarthritis: T_2, T_1 rho, dGEMRIC and contrast-enhanced computed tomography. Magn Reson Imaging 2009;27:779–84.

34. Dardzinski BJ, Mosher TJ, Li S, Van Slyke MA, Smith MB. Spatial variation of T_2 in human articular cartilage. Radiology 1997;205:546–50.

35. Dunn TC, Lu Y, Jin H, Ries MD, Majumdar S. T_2 relaxation time of cartilage at MR imaging: comparison with severity of knee osteoarthritis. Radiology 2004;232:592–8.

36. Stehling C, Liebl H, Krug R, Lane NE, Nevitt MC, Lynch J, et al. Patellar cartilage: T_2 values and morphologic abnormalities at 3.0-T MR imaging in relation to physical activity in asymptomatic subjects from the osteoarthritis initiative. Radiology 2010;254:509–20.

37. Xia Y. Relaxation anisotropy in cartilage by NMR microscopy (muMRI) at 14-mum resolution. Magn Reson Med 1998;39:941–9.

38. Xia Y, Moody JB, Alhadlaq H. Orientational dependence of T_2 relaxation in articular cartilage: a microscopic MRI (muMRI) study. Magn Reson Med 2002;48:460–9.

39. Nissi MJ, Rieppo J, Töyräs J, Laasanen MS, Kiviranta I, Jurvelin JS, et al. T_2 relaxation time mapping reveals age- and species-related diversity of collagen network architecture in articular cartilage. Osteoarthritis Cartilage 2006;14:1265–71.

40. Shapiro EM, Borthakur A, Kaufman JH, Leigh JS, Reddy R. Water distribution patterns inside bovine articular cartilage as visualized by ^{1}H magnetic resonance imaging. Osteoarthritis Cartilage 2001;9:533–8.

41. Wayne JS, Kraft KA, Shields KJ, Yin C, Owen JR, Disler DG. MR imaging of normal and matrix-depleted cartilage: correlation with biomechanical function and biochemical composition. Radiology 2003;228:493–9.

42. Benjamin M, Milz S, Bydder GM. Magnetic resonance imaging of entheses. Part 1. Clin Radiol 2008;63:691–703.

43. Williams A, Qian Y, Bear D, Chu CR. Assessing degeneration of human articular cartilage with ultra-short echo time (UTE) $T_2^\star$ mapping. Osteoarthritis Cartilage 2010;18:539–46.

44. Borthakur A, Mellon E, Niyogi S, Witschey W, Kneeland JB, Reddy R. Sodium and T_1rho MRI for molecular and diagnostic imaging of articular cartilage. NMR Biomed 2006;19:781–821.

45. Duvvuri U, Reddy R, Patel SD, Kaufman JH, Kneeland JB, Leigh JS. $T_{1\rho}$-relaxation in articular cartilage: effects of enzymatic degradation. Magn Reson Med 1997;38:863–7.

46. Pakin SK, Schweitzer ME, Regatte RR. 3D-T_1rho quantitation of patellar cartilage at 3.0T. J Magn Reson Imaging 2006;24:1357–63.

47. Li X, Han ET, Busse RF, Majumdar S. In vivo T_1rho mapping in cartilage using 3D magnetization-

prepared angle-modulated partitioned k-space spoiled gradient echo snapshots (3D MAPSS). Magn Reson Med 2008;59: 298–307.

48. Akella SVS, Regatte RR, Gougoutas AJ, Borthakur A, Shapiro EM, Kneeland JB, et al. Proteoglycan-induced changes in T_1 rho-relaxation of articular cartilage at 4T. Magn Reson Med 2001;46: 419–23.

49. Witschey WRT, Borthakur A, Fenty M, Kneeland BJ, Lonner JH, McArdle EL, et al. T_1rho MRI quantification of arthroscopically confirmed cartilage degeneration. Magn Reson Med 2010;63: 1376–82.

50. Holtzman DJ, Theologis AA, Carballido-Gamio J, Majumdar S, Li XJ, Benjamin C. T_1 rho and T-2 quantitative magnetic resonance imaging analysis of cartilage regeneration following microfracture and mosaicplasty cartilage resurfacing procedures. J Magn Reson Imaging 2010;32:914–23.

51. Li X, Benjamin Ma C, Link TM, Castillo DD, Blumenkrantz G, Lozano J, et al. In vivo $T_1[\text{rho}]$ and T_2 mapping of articular cartilage in osteoarthritis of the knee using 3 T MRI. Osteoarthritis Cartilage 2007;15:789–97.

52. Regatte RR, Akella SVS, Borthakur A, Kneeland JB, Reddy R. Proteoglycan depletion-induced changes in transverse relaxation maps of cartilage: comparison of T_2 and $T_1[\text{rho}]$. Acad Radiol 2002;9:1388–94.

53. Regatte RR, Akella SVS, Lonner JH, Kneeland JB, Reddy R. T_1rho relaxation mapping in human osteoarthritis (OA) cartilage: comparison of T_1rho with T_2. J Magn Reson Imaging 2006;23: 547–53.

54. Akella SVS, Regatte RR, Wheaton AJ, Borthakur A, Reddy R. Reduction of residual dipolar interaction in cartilage by spin-lock technique. Magn Reson Med 2004;52:1103–9.

55. Menezes NM, Gray ML, Hartke JR, Burstein D. T_2 and T_1rho MRI in articular cartilage systems. Magn Reson Med 2004;51:503–9.

56. Schick F. Whole-body MRI at high field: technical limits and clinical potential. Eur Radiol 2005;15:946–59.

57. Katta J, Jin Z, Ingham E, Fisher J. Biotribology of articular cartilage —a review of the recent advances. Med Eng Phys 2008;30:1349–63.

58. Kleemann RU, Krocker D, Cedraro A, Tuischer J, Duda GN. Altered cartilage mechanics and histology in knee osteoarthritis: relation to clinical assessment (ICRS Grade). Osteoarthritis Cartilage 2005;13:958–63.

59. Juras V, Bittsansky M, Majdisova Z, Szomolanyi P, Sulzbacher I, Gabler S, et al. In vitro determination of biomechanical properties of human articular cartilage in osteoarthritis using multi-parametric MRI. J Magn Reson 2009;197:40–7.

60. Wheaton AJ, Dodge GR, Elliott DM, Nicoll SB, Reddy R. Quantification of cartilage biomechanical and biochemical properties via $T_{1\rho}$ magnetic resonance imaging. Magn Reson Med 2005;54: 1087–93.

61. Saarakkala S, Julkunen P, Kiviranta P, Mäkitalo J, Jurvelin JS, Korhonen RK. Depth-wise progression of osteoarthritis in human articular cartilage: investigation of composition, structure and biomechanics. Osteoarthritis Cartilage 2010;18: 73–81.

62. Granot J. Sodium imaging of human body organs and extremities in vivo. Radiology 1988;167: 547–50.

63. Grobner T. Gadolinium—a specific trigger for the development of nephrogenic fibrosing dermopathy and nephrogenic systemic fibrosis? Nephrol Dial Transplant 2006;21:1104–8.

64. Reddy R, Insko EK, Noyszewski EA, Dandora R, Kneeland JB, Leigh JS. Sodium MRI of human articular cartilage in vivo. Magn Reson Med 1998;39: 697–701.

65. Borthakur A, Shapiro EM, Beers J, Kudchodkar S, Kneeland JB, Reddy R. Sensitivity of MRI to proteoglycan depletion in cartilage: comparison of sodium and proton MRI. Osteoarthritis Cartilage 2000;8:288–93.

66. Shapiro EM, Borthakur A, Gougoutas A, Reddy R. ^{23}Na MRI accurately measures fixed charge density in articular cartilage. Magn Reson Med 2002;47: 284–91.

67. Robson MD, Gatehouse PD, Bydder M, Bydder GM. Magnetic resonance: an introduction to ultrashort TE (UTE) imaging. J Comput Assist Tomogr 2003;27: 825–46.

68. Nielles-Vallespin S, Weber M-A, Bock M, Bongers A, Speier P, Combs SE, et al. 3D radial projection technique with ultrashort echo times for sodium MRI: clinical applications in human brain and skeletal muscle. Magn Reson Med 2007;57:74–81.

69. Wang LG, Wu Y, Chang G, Oesingmann N, Schweitzer ME, Jerschow A, et al. Rapid isotropic 3D-sodium MRI of the knee joint in vivo at 7T. J Magn Reson Imaging 2009;30:606–14.

70. Wolff SD, Balaban RS. Magnetization transfer contrast (MTC) and tissue water proton relaxation in vivo. Magn Reson Med 1989; 10:135–44.

71. Lin P-C, Reiter DA, Spencer RG. Sensitivity and specificity of univariate MRI analysis of experimentally degraded cartilage. Magn Reson Med 2009;62:1311–18.

72. Regatte RR, Akella SVS, Reddy R. Depth-dependent proton magnetization transfer in articular cartilage. J Magn Reson Imaging 2005;22:318–23.

73. Gray ML, Burstein D, Lesperance LM, Gehrke L. Magnetization transfer in cartilage and its constituent macromolecules. Magn Reson Med 1995;34:319–25.

74. Wachsmuth L, Juretschke HP, Raiss RX. Can magnetization transfer magnetic resonance imaging follow proteoglycan depletion in articular cartilage? MAGMA 1997;5:71–8.

75. Li W, Hong L, Hu L, Magin RL. Magnetization transfer imaging provides a quantitative measure of chondrogenic differentiation and tissue development. Tissue Eng Part C Methods 2010;16: 1407–15.

76. Yao WW, Qu N, Lu ZH, Yang SX. The application of T_1 and T_2 relaxation time and magnetization transfer ratios to the early diagnosis of patellar cartilage osteoarthritis. Skeletal Radiol 2009;38: 1055–62.

77. van Zijl PCM, Yadav NN. Chemical exchange saturation transfer (CEST): what is in a name and what isn't? Magn Reson Med 2011;65:927–48.

78. Ward KM, Aletras AH, Balaban RS. A new class of contrast agents for MRI based on proton chemical exchange dependent saturation transfer (CEST). J Magn Reson 2000;143:79–87.

79. Ling W, Regatte RR, Navon G, Jerschow A. Assessment of glycosaminoglycan concentration in vivo by chemical exchange-dependent saturation transfer (gagCEST). Proc Natl Acad Sci USA 2008;105:2266–70.

80. Schmitt B, Zbýň Š, Stelzeneder D, Jellus V, Paul D, Lauer L, et al. Cartilage quality assessment by using glycosaminoglycan chemical exchange saturation transfer and 23Na MR imaging at 7 T. Radiology 2011;260:257–64.

81. Freeman R. Magnetic resonance in chemistry and medicine. Oxford, UK: Oxford University Press; 2003.

82. Stejskal EO, Tanner JE. Spin diffusion measurements: spin echoes in the presence of a time-dependent field gradient. J Chem Phys 1965;42:288–92.

83. Mattiello J, Basser PJ, Lebihan D. Analytical expressions for the b-matrix in NMR diffusion imaging and spectroscopy. J Magn Reson Ser A 1994;108:131–41.

84. Burstein D, Gray ML, Hartman AL, Gipe R, Foy BD. Diffusion of small solutes in cartilage as measured by nuclear magnetic resonance (NMR) spectroscopy and imaging. J Orthop Res 1993;11: 465–78.

85. Mlynárik V, Sulzbacher I, Bittšanský M, Fuiko R, Trattnig S. Investigation of apparent diffusion constant as an indicator of early degenerative disease in articular cartilage. J Magn Reson Imaging 2003;17:440–4.

86. Miller KL, Hargreaves BA, Gold GE, Pauly JM. Steady-state diffusion-weighted imaging of in vivo knee cartilage. Magn Reson Med 2004;51:394–8.

87. Mamisch TC, Menzel MI, Welsch GH, Bittersohl B, Salomonowitz E, Szomolanyi P, et al. Steady-state diffusion imaging for MR in-vivo evaluation of reparative cartilage after matrix-associated autologous chondrocyte transplantation at 3 tesla—preliminary results. Eur J Radiol 2008;65:72–9.

88. Friedrich KM, Mamisch TC, Plank C, Langs G, Marlovits S, Salomonowitz E, et al. Diffusion-weighted imaging for the follow-up of patients after matrix-associated autologous chondrocyte transplantation. Eur J Radiol 2010;73:622–8.

89. Meder R, de Visser SK, Bowden JC, Bostrom T, Pope JM. Diffusion tensor imaging of articular cartilage as a measure of tissue microstructure. Osteoarthritis Cartilage 2006;14:875–81.

90. de Visser SK, Crawford RW, Pope JM. Structural adaptations in compressed articular cartilage measured by diffusion tensor imaging. Osteoarthritis Cartilage 2008;16:83–9.

91. Pierce DM, Trobin W, Raya JG, Trattnig S, Bischof H, Glaser C, et al. DT-MRI based computation of collagen fiber deformation in human articular cartilage: a feasibility study. Ann Biomed Eng 2010;38:2447–63.

92. Tan AL, Toumi H, Benjamin M, Grainger AJ, Tanner SF, Emery P, et al. Combined high-resolution magnetic resonance imaging and histological examination to explore the role of ligaments and tendons in the phenotypic expression of early hand osteoarthritis. Ann Rheum Dis 2006;65: 1267–72.

93. Tan AL, Grainger AJ, Tanner SF, Shelley DM, Pease C, Emery P, et al. High-resolution magnetic

resonance imaging for the assessment of hand osteoarthritis. Arthritis Rheum 2005;52:2355–65.

94. Benjamin M, Bydder GM. Magnetic resonance imaging of entheses using ultrashort TE (UTE) pulse sequences. J Magn Reson Imaging 2007;25:381–9.

95. Benjamin M, McGonagle D. Histopathologic changes at "synovio–entheseal complexes" suggesting a novel mechanism for synovitis in osteoarthritis and spondylarthritis. Arthritis Rheum 2007;56:3601–9.

96. Benjamin M, Milz S, Bydder GM. Magnetic resonance imaging of entheses. Part 2. Clin Radiol 2008; 63:704–11.

97. Blamire AM. The technology of MRI—the next 10 years? Br J Radiol 2008;81:601–17.

98. Gatehouse PD, Bydder GM. Magnetic resonance imaging of short T_2 components in tissue. Clin Radiol 2003;58:1–19.

99. Springer F, Martirosian P, Machann J, Schwenzer NF, Claussen CD, Schick F. Magnetization transfer contrast imaging in bovine and human cortical bone applying an ultrashort echo time sequence at 3 Tesla. Magn Reson Med 2009;61:1040–8.

100. McGonagle D, Tan AL, Carey J, Benjamin M. The anatomical basis for a novel classification of osteoarthritis and allied disorders. J Anat 2010;216: 279–91.

101. Brandt KD, Radin EL, Dieppe PA, van dePutte L. Yet more evidence that osteoarthritis is not a cartilage disease. Ann Rheum Dis 2006;65:1261–4.